



## RESEARCH ARTICLE

10.1029/2020JD033137

### Key Points:

- First study to measure a comprehensive set of ozone-depleting substances in air entering the stratosphere above the Asian summer monsoon
- Higher than expected mixing ratios found for many compounds, particularly chlorinated very short-lived substances
- Regional estimate but the extra equivalent chlorine could significantly enhance the chlorine and bromine loading of the entire stratosphere

### Supporting Information:

- Supporting Information S1

### Correspondence to:






K. E. Adcock,  
[Karina.Adcock@uea.ac.uk](mailto:Karina.Adcock@uea.ac.uk)

### Citation:

Adcock, K. E., Fraser, P. J., Hall, B. D., Langenfelds, R. L., Lee, G., Montzka, S. A., et al. (2021). Aircraft-based observations of ozone-depleting substances in the upper troposphere and lower stratosphere in and above the Asian summer monsoon. *Journal of Geophysical Research: Atmospheres*, 126, e2020JD033137. <https://doi.org/10.1029/2020JD033137>

Received 21 MAY 2020  
 Accepted 30 NOV 2020

## Aircraft-Based Observations of Ozone-Depleting Substances in the Upper Troposphere and Lower Stratosphere in and Above the Asian Summer Monsoon

Karina E. Adcock<sup>1</sup> , Paul J. Fraser<sup>2</sup>, Brad D. Hall<sup>3</sup>, Ray L. Langenfelds<sup>2</sup> , Geoffrey Lee<sup>1</sup>, Stephen A. Montzka<sup>3</sup> , David E. Oram<sup>1,4</sup>, Thomas Röckmann<sup>5</sup>, Fred Stroh<sup>6</sup> , William T. Sturges<sup>1</sup>, Bärbel Vogel<sup>6</sup>, and Johannes C. Laube<sup>1,6</sup> 

<sup>1</sup>Centre for Ocean and Atmospheric Sciences, School of Environmental Sciences, University of East Anglia, Norwich, UK, <sup>2</sup>Oceans and Atmosphere, Climate Science Centre, Commonwealth Scientific and Industrial Research Organisation, Aspendale, VIC, Australia, <sup>3</sup>Global Monitoring Laboratory, National Oceanic and Atmospheric Administration, Boulder, CO, USA, <sup>4</sup>National Centre for Atmospheric Science, School of Environmental Sciences, University of East Anglia, Norwich, UK, <sup>5</sup>Institute for Marine and Atmospheric Research, Utrecht University, Utrecht, The Netherlands, <sup>6</sup>Institute of Energy and Climate Research – Stratosphere (IEK-7), Jülich, Germany

**Abstract** Recent studies show that the Asian summer monsoon anticyclone (ASMA) transports emissions from the rapidly industrializing nations in Asia into the tropical upper troposphere. Here, we present a unique set of measurements on over 100 air samples collected on multiple flights of the M55 Geophysica high altitude research aircraft over the Mediterranean, Nepal, and Northern India during the summers of 2016 and 2017 as part of the European Union project StratoClim. These air samples were measured for 27 ozone-depleting substances (ODSs), many of which were enhanced above expected levels, including the chlorinated very short-lived substances, dichloromethane (CH<sub>2</sub>Cl<sub>2</sub>), 1,2-dichloroethane (CH<sub>2</sub>ClCH<sub>2</sub>Cl), and chloroform (CHCl<sub>3</sub>). CH<sub>2</sub>Cl<sub>2</sub> mixing ratios in the tropopause region were 65–136 parts per trillion (ppt) in comparison to previous estimates of mixing ratios in the tropical tropopause layer of 30–44 ppt in 2013–2014. Backward trajectories, calculated with the trajectory module of the chemistry-transport model CLaMS and driven by the ERA5 reanalysis, indicate possible source regions of CH<sub>2</sub>Cl<sub>2</sub> in South Asia. We derived total equivalent chlorine (ECI), and equivalent effective stratospheric chlorine (EESC) and found that these quantities were substantially higher than previous estimates in the literature. EESC at mean age-of-air of 3 years based on the 2016 measurements was 1,861–1,872 ppt in comparison to a previously estimated EESC of 1,646 ppt. Our findings show that the ASMA transports larger than expected mixing ratios of long-lived and very short-lived ODSs into the upper troposphere and lower stratosphere, likely leading to an impact on the stratospheric ozone layer.

**Plain Language Summary** The Asian summer monsoon is an enormous weather system that occurs every summer over large parts of the Asian continent. It is known to transport emissions from the rapidly industrializing nations in East and South Asia into the tropical upper troposphere, but how much of that enters the stratosphere above is not well-known. Here, we present a unique set of measurements on over 100 air samples collected in regions directly influenced by this monsoon system. The flights of a high altitude research aircraft took place during the summers of 2016 and 2017. These air samples were investigated for their content of ozone-depleting substances (ODSs), which are known to be involved in the depletion of the life-protecting stratospheric ozone layer. Many of the ODSs were enhanced above expected levels, including the particularly understudied very short-lived chlorine-containing compounds, dichloromethane (CH<sub>2</sub>Cl<sub>2</sub>), 1,2-dichloroethane (CH<sub>2</sub>ClCH<sub>2</sub>Cl), and chloroform (CHCl<sub>3</sub>). An analysis of the air mass origins indicated fast transport times and source regions in South Asia. Our findings show that the Asian monsoon is transporting larger than expected mixing ratios of ODSs into the upper troposphere and lower stratosphere, likely leading to an impact on the stratospheric ozone layer.

## 1. Introduction

The Asian summer monsoon anticyclone (ASMA) occurs during the boreal summer (July, August, and September) over East and South Asia. It is a major meteorological system characterized by deep convection and anticyclonic flow in the upper troposphere and lower stratosphere (UTLS) and is subject to strong

© 2020. The Authors.

This is an open access article under the terms of the [Creative Commons Attribution License](https://creativecommons.org/licenses/by/4.0/), which permits use, distribution and reproduction in any medium, provided the original work is properly cited.

dynamical variability (e.g., Garny & Randel, 2013; Q. Li et al., 2005; Park et al., 2008, 2009, 2007; Randel & Park, 2006; Vogel et al., 2015). Within the ASMA, air masses are rapidly uplifted from the boundary layer into the UTLS (e.g., Brunamonti et al., 2018; Park et al., 2009; Randel et al., 2010).

In this study, we investigate whether the Asian summer monsoon convection transports elevated levels of ozone-depleting substances (ODSs) including very short-lived substances (VSLs) into the lower stratosphere. VSLs are defined here as having atmospheric lifetimes of 6 months or less (Engel, Rigby et al., 2018b). VSLs are not regulated under the Montreal Protocol on Substances that Deplete the Ozone Layer and have large sinks in the troposphere, which limits their contribution to stratospheric ozone depletion. However, the ASMA provides an effective pathway to transport air containing tropospheric trace gases from the surface into the lower stratosphere on the time scale of a few days to a few weeks. Thus, VSLs emitted from surface regions in the ASMA should be able to reach the stratosphere at significantly elevated mixing ratios (e.g., Brioude et al., 2010; Hossaini et al., 2016; Orbe et al., 2015; Tissier & Legras, 2016; Vogel et al., 2014, 2019).

The tropics are the main entrance region to the stratosphere associated with the large-scale Brewer-Dobson circulation. Transport via the ASMA provides an additional seasonal source of air into the global stratosphere, especially into the northern hemispheric lower stratosphere (Orbe et al., 2016; Ploeger et al., 2017; Vogel et al., 2016). Convection uplifts air over polluted regions, such as the Indian subcontinent and South-East Asia and this air is then horizontally confined in the UTLS by the anticyclonic winds (e.g., Park et al., 2007; Ploeger et al., 2015; Vogel et al., 2015). Then air in the ASMA is transported either vertically toward the tropical stratosphere or quasihorizontally into the Northern Hemisphere extratropical lower stratosphere (e.g., Garny & Randel, 2016; Orbe et al., 2015; Ploeger et al., 2017; Vogel et al., 2016, 2019).

Using the model-based results of Ploeger et al. (2017) it can be estimated that, on an annual average basis, air from the ASMA contributes about 5% of the air in the Northern Hemisphere extratropical stratosphere (at a potential temperature level of 380 K), whereas in the tropical stratosphere the contribution is about 2% in the tropical pipe (at 460 K) and in the Southern Hemisphere extratropical stratosphere less than 0.5% (at 380 K, Ploeger et al., 2017). The maximum contribution of air from the Asian monsoon anticyclone in the Northern Hemispheric lower stratosphere is found during autumn and is around 15% (Ploeger et al., 2017). The transport of ODSs from the ASMA region into the Northern Hemisphere extratropical lower stratosphere therefore has the potential to change the chemical composition of this part of the atmosphere. In addition, it has recently been found that ozone at mid-latitudes in the lower stratosphere is still decreasing, and although this is an ongoing discussion, it has been suggested that VSLs may be one of the factors contributing to this (Ball et al., 2018; Chipperfield et al., 2018; Hossaini et al., 2015).

The contribution of chlorinated VSLs to total chlorine at the surface increased in recent years, from an average rate of around  $\sim 2.5$  ppt Cl yr<sup>-1</sup> (2004–2012) to  $\sim 4.3 \pm 4.9$  ppt Cl yr<sup>-1</sup> (2012–2016; Engel, Rigby et al., 2018b) and could continue to increase in the future (Fang et al., 2019; Feng et al., 2018; Leedham Elvidge et al., 2015; Oram et al., 2017). Total tropospheric chlorine has been decreasing in recent years due to the Montreal Protocol. However, this rate of decrease is slowing down: from  $11.8 \pm 6.9$  ppt Cl yr<sup>-1</sup> during 2008–2012 to  $4.4 \pm 4.1$  ppt Cl yr<sup>-1</sup> during 2012–2016 (Engel, Rigby et al., 2018b). This is due, in part, to increasing mixing ratios of chlorinated VSLs, in particular, in East and South-East Asia (Claxton et al., 2020; Engel, Rigby et al., 2018b; Fang et al., 2019). This could undermine some of the progress made by the Montreal Protocol and its amendments and further offset the reduction in emissions and mixing ratios of long-lived ODSs.

The three major chlorinated VSLs are dichloromethane (CH<sub>2</sub>Cl<sub>2</sub>), 1,2-dichloroethane (CH<sub>2</sub>ClCH<sub>2</sub>Cl), and chloroform (trichloromethane; CHCl<sub>3</sub>; Engel, Rigby et al., 2018b). CHCl<sub>3</sub> and CH<sub>2</sub>Cl<sub>2</sub> are usually coproduced industrially (McCulloch, 2017). CH<sub>2</sub>Cl<sub>2</sub> has an atmospheric lifetime of about 6 months and its global atmospheric abundances are believed to be at least 90% anthropogenic in origin in recent years (Claxton et al., 2020; Engel, Rigby et al., 2018b). It has a wide range of industrial applications in chemical and pharmaceutical processes and in the production of HFC-32 (CH<sub>2</sub>F<sub>2</sub>; McCulloch, 2017). CHCl<sub>3</sub> has an atmospheric lifetime of about 6 months and is estimated to be about 50% anthropogenic in origin (Engel, Rigby et al., 2018b). The principal use for CHCl<sub>3</sub> is as a chemical feedstock for the production of HCFC-22 (CHClF<sub>2</sub>; Oram et al., 2017). CH<sub>2</sub>ClCH<sub>2</sub>Cl has an atmospheric lifetime of about 3 months and it is likely

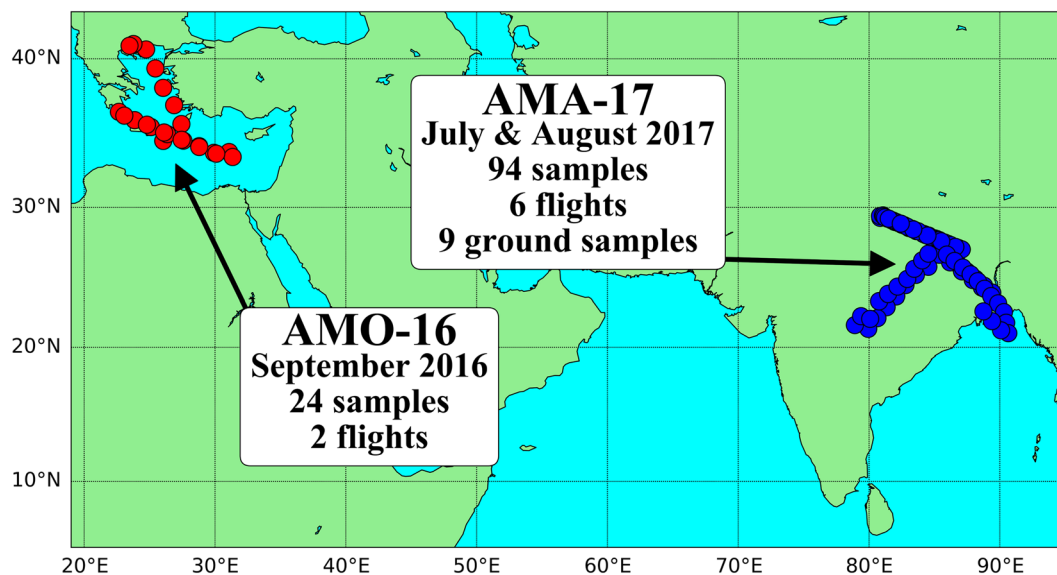


**Figure 1.** The latitude and longitude locations where air samples were collected on board the Geophysica research aircraft during the AMO-16 (red) and AMA-17 (blue) campaigns.

fully anthropogenic in origin (Engel, Rigby et al., 2018b). Its primary use is in the manufacture of vinyl chloride, the precursor to polyvinyl chloride, and other chlorinated solvents (Oram et al., 2017). It is likely that there are major source regions of these chlorinated VSLs in China and India (Claxton et al., 2020; Fang et al., 2019; Oram et al., 2017; Say et al., 2019).

Recent studies, using air samples collected at ground-based measurement sites and on board aircraft at altitudes of 0.02–12 km, found enhancements of chlorinated VSLs in the South and East Asian region, both at the surface and in the lower and upper troposphere (Leedham Elvidge et al., 2015; Oram et al., 2017; Say et al., 2019). Upper tropospheric levels of these chlorinated VSLs are likely to ascend into the lower stratosphere. This is supported by satellite observations of unusually high levels of phosgene ( $\text{COCl}_2$ ) in the stratosphere, a product gas of the photochemical decomposition of  $\text{CH}_2\text{Cl}_2$ ,  $\text{CHCl}_3$ , and other gases (Harrison et al., 2019). Our study investigates this hypothesis with air samples collected via a high-altitude research aircraft in the ASMA region but at higher altitudes (up to 20 km), that is, within the lower stratosphere where no in situ data exists for many ODSs.

## 2. Methods

### 2.1. Aircraft Campaigns

Air samples were collected during two campaigns of the M55 Geophysica high-altitude research aircraft that were part of the StratoClim EU project ([www.stratoclim.org](http://www.stratoclim.org)). Sample collection and measurement details such as coordinates, altitudes, pressures, potential temperatures, and mixing ratios of various trace gases can be found in the supporting information.

The first campaign took place over the Mediterranean in September 2016. The aim of this campaign was to measure the composition of the outflow from the ASMA. The monsoon circulation system has a large variability in its spatial extent and can reach from the Mediterranean and North-East Africa to East Asia (Annamalai & Slingo, 2001; Garny & Randel, 2013; Pan et al., 2016; Vogel et al., 2015). This campaign is referred to as AMO-16 (the Asian Monsoon Outflow 2016 campaign). During AMO-16, 24 air samples were collected during two flights (September 1 and 6, 2016). The aircraft operated from Kalamata, Greece (37.1°, 22.0°) and samples were collected in the region of 33°N–41°N, 23°E–31°E, 10–20 km altitude (Figure 1).

The second campaign took place over the Indian subcontinent in July–August 2017. The aim of this campaign was to measure the composition of the ASMA. This campaign is referred to as AMA-17 (the Asian

Monsoon Anticyclone 2017 campaign). During AMA-17, 94 samples were collected during six flights (July 27, 2017, July 29, 2017, July 31, 2017, August 2, 2017, August 4, 2017, and August 6, 2017). The campaign base was Tribhuvan International Airport at Kathmandu, Nepal (27.7°, 85.4°) and samples were collected in the region of 21°N–29°N, 79°E–91°E, 10–20 km altitude (Figure 1). In addition to the flight samples, nine air samples were collected at ground level, two samples at Kathmandu University and the rest at Kathmandu airport. Kathmandu is situated at an elevation of about 1,400 m.

## 2.2. Analytical Technique

Air samples were collected with the whole air sampler of Utrecht University operated on board the Geophysica research aircraft (Cairo et al., 2010; Kaiser et al., 2006; Laube, Engel, et al., 2010a). Ambient air was compressed into evacuated stainless-steel canisters (2 L) using a metal bellows pump that has been previously shown to not impact trace gas mixing ratios (Laube, Engel, et al., 2010a). In addition, for AMA-17 the internal surfaces of 30 canisters were passivated using a common passivation technique (“Silco™-treatment”) to minimize the breakdown of more reactive gases in the canisters between collection and analysis (25 filled on board the aircraft and 5 at ground level).

The samples were transported to the University of East Anglia (UEA) for analysis on a high sensitivity gas chromatograph—tri-sector mass spectrometer system (Waters AutoSpec GC-MS). The trace gases were cryogenically extracted and preconcentrated. A full description of this system can be found in Laube, Martinier, et al. (2010b). The different compounds were separated on a GS-GasPro column (length ~ 50 m; ID: 0.32 mm). In addition, all of the AMO-16 and some of the AMA-17 samples were reanalyzed on a KCl-passivated CP-PLOT Al<sub>2</sub>O<sub>3</sub> column (length: 50 m; ID: 0.32 mm; Laube et al., 2016). During analysis on the Al<sub>2</sub>O<sub>3</sub> column, an Ascarite (NaOH-coated silica) trap was used to remove carbon dioxide, which can distort or reduce the signal of a number of compounds. A full list of measured species and their calibration scales can be found in Table S1.

All samples were bracketed by measurements of a working standard (in AMO-16: AAL-071170 and in AMA-17: SX-3591). Calibrations of our target compounds in these working standards were in part provided by the National Oceanic and Atmospheric Administration's Global Monitoring Laboratory in Boulder, USA and complemented by UEA internal calibrations for some gases. UEA intercomparisons of these working standards with four other working standards, two of which had internal surfaces of passivated aluminum, were used to ensure that results were consistent over time and in relation to long-term tropospheric trends. It was confirmed that the mixing ratios of all compounds presented here remained constant in the two primary working standards within three standard deviations during the 2008–2017 period, except for methyl bromide (CH<sub>3</sub>Br) in the SX-3591 standard. This is likely to be due to loss (absorption and/or breakdown) of CH<sub>3</sub>Br on the internal walls of the cylinders and CH<sub>3</sub>Br mixing ratios for SX-3591 were drift-corrected accordingly (see supporting information). The dry-air mole fractions (mixing ratios) were measured for 27 ODSs (Table S1), and the unit, parts per trillion (ppt), is used in this study as an equivalent to picomole per mole. Some additional non-ODSs were measured that are good tracers for stratospheric mean age-of-air calculations and can be used to derive tropospheric emissions, including sulfur hexafluoride (SF<sub>6</sub>), perfluoroethane (C<sub>2</sub>F<sub>6</sub>), HFC-125 (CHF<sub>2</sub>CF<sub>3</sub>), and HFC-32 (CH<sub>2</sub>F<sub>2</sub>).

Due to potential loss during storage for some of the compounds of interest, the time between flask collection and measurement was kept as short as possible. During AMO-16, the time between collection and measurement was 14–19 days. During AMA-17, the time between collection and measurement was more variable between 2 and 8 weeks/16–54 days. Only CCl<sub>4</sub> (carbon tetrachloride, tetrachloromethane) and CH<sub>3</sub>Cl (methyl chloride, chloromethane) were affected by the longer time delay in AMA-17 and for these compounds, the samples that were measured later and were not stored in Silco™-treated canisters have been removed from the analysis. CCl<sub>4</sub> had previously been found to be unstable in stainless steel canisters containing dry air over long periods (Laube et al., 2008, 2013). For more information on this see supporting information.

## 2.3. Chemical Lagrangian Model of the Stratosphere Backward Trajectory Calculations

There are multiple factors that influence the mixing ratios of VSLs in the UTLS: the emissions near the surface, the time taken for air to be transported from the surface to the UTLS (i.e., convection), and the mixing

processes in the troposphere and the stratosphere. In order to investigate the possible source regions of enhanced  $\text{CH}_2\text{Cl}_2$  mixing ratios, 10-day backward trajectories were calculated for each sample collected during AMA-17 using the trajectory module of the Chemical Lagrangian Model of the Stratosphere (CLaMS; Konopka et al., 2012; McKenna, 2002; Pommrich et al., 2014; and references therein). Only trajectories for AMA-17 were calculated, as AMO-16 samples that were influenced by the ASMA have much longer transport times from  $\text{CH}_2\text{Cl}_2$  sources in Asia to the location of the measurements at UTLS altitudes in the Mediterranean area. Therefore, they will have experienced more mixing and chemical break down and so will have a more diluted source signal than AMA-17 samples. This is in agreement with the lower mixing ratios of most compounds in AMO-16 in comparison to AMA-17. In addition, only AMA-17 samples measured at potential temperatures of less than 390 K were used for backward trajectory calculations, that is, 53 out of 94 samples, because we focus here on enhanced mixing ratios of  $\text{CH}_2\text{Cl}_2$ .

The CLaMS backward trajectory calculations are driven by horizontal winds from the high-resolution ERA5 reanalysis (Hersbach et al., 2020) recently released by the European Center for Medium-Range Weather Forecasts. ERA5 provides data on a  $0.3 \times 0.3$  horizontal grid every hour on 137 hybrid levels from the surface to 0.01 hPa. In general, this results in a much better representation of convective updrafts and tropical cyclones in ERA5 (e.g., Hoffmann et al., 2019; Li et al., 2020; Legras & Bucci, 2020) compared with the earlier ERA-Interim reanalysis (Dee et al., 2011). To derive the vertical velocities, we used diabatic heating rates including latent heat release (for details, see Ploeger et al., 2010).

The CLaMS model trajectory calculations were used to find the last location the air parcel was in the model boundary layer (trajectory end point). The model boundary layer was set to  $\approx 2\text{--}3$  km above the surface following orography (for more details see Vogel et al., 2015). The location of trajectory end points provides an indication of the regions where surface sources last influenced the mixing ratios measured in the air samples. Each air sample typically took 2–3 min to be collected. To investigate the variability of the trajectories within the whole time interval of the measurements, ERA5-based CLaMS backward trajectories were calculated every second for the entire time interval over which an air sample was collected during the flight.

#### 2.4. Equivalent Chlorine

Equivalent chlorine (ECl) is the sum of the mixing ratios of chlorine and bromine atoms from all halogen source gases; the bromine mixing ratios are multiplied by a weighting factor of 60 as bromine is about 60–65 times more effective at depleting ozone than chlorine (Daniel et al., 2007; Sinnhuber et al., 2009). The ECl calculation was used to investigate the eventual impact on stratospheric ozone of ODSs measured in the tropopause region of the ASMA in comparison to estimates of ECl based on measurements in other atmospheric regions.

#### 2.5. Equivalent Effective Stratospheric Chlorine

The Equivalent Effective Stratospheric Chlorine (EESC) is defined as the “chlorine-equivalent sum of chlorine and bromine derived from ODS tropospheric abundances, weighted to reflect their expected depletion of stratospheric ozone” (Engel, Rigby et al., 2018b). EESC—like the ECl—takes into account the sum of the mixing ratios of chlorine and bromine atoms from all halogen source gases with bromine multiplied by 60. However, EESC—in contrast to ECl—takes into account the effects of stratospheric transport and chemistry on the amount of chlorine and bromine released from long-lived ODSs at a given location and time.

As stratospheric circulation is slow, air sampled in the stratosphere may have entered it several years ago. The “mean age-of-air” is defined as the average amount of time an air parcel has spent in the stratosphere. Inert compounds can be used as “age-of-air tracers” to calculate the “mean age-of-air” of the air sampled in the stratosphere provided that there are (a) long-term measurements of their global tropospheric mixing ratios and (b) these mixing ratios have been monotonically increasing over time at sufficient rates. Our mean age calculation also takes into account the underlying transit time distribution (the “age spectrum”) using the parameterization introduced by Engel et al. (2002).

The mean ages-of-air were calculated using ground-level background mixing ratio trends of selected gases from 1978 to January 2018 from air samples collected at the Cape Grim, Tasmania ( $40.7^\circ\text{S}$ ,  $144.7^\circ\text{E}$ )



baseline station and analyzed at the UEA (Laube, Martinerie et al., 2010b, 2013). These mixing ratio trends were shifted backwards in time by 6 months, which has been proven to be a good proxy for air entering the stratosphere via the upper troposphere in the tropics, provided the gas is inert enough in the troposphere, (i.e., no significant decomposition on tropospheric transport time scales; Leedham Elvidge et al., 2018). Commonly used age-of-air tracers include sulfur hexafluoride ( $\text{SF}_6$ ) and carbon dioxide ( $\text{CO}_2$ ; e.g., Andrews et al., 2001; Engel et al., 2002; Volk et al., 1997). However, recent research has introduced other potential age tracers (Leedham Elvidge et al., 2018). We compared three different age-of-air tracers:  $\text{SF}_6$ ,  $\text{C}_2\text{F}_6$ , and HFC-125 in air samples collected during AMO-16 and AMA-17. The mean ages of air were then calculated using the same methods described in Leedham Elvidge et al. (2018). For more information, see [Supporting Information Material](#).

For trace gases with stratospheric sinks such as ODSs, at mid-latitudes a mean age of 3 years is generally used as a reference to estimate the EESC in that region (Engel, Rigby et al., 2018b). The mixing ratios of ODSs measured in the stratosphere at a mean age-of-air of 3 years, for example, would be roughly similar to their mixing ratios in the upper troposphere 3 years earlier, assuming no decomposition. As ODSs are at least partly broken down by strong UV radiation and/or reaction with OH radicals and  $\text{O}(^1\text{D})$  in the stratosphere, the mixing ratios of these compounds are however impacted not just by the age of the air but also by different reactions and reaction rates.

For long-lived ODSs, similarly time-shifted tropospheric trends from Cape Grim were propagated into the stratosphere and mixing ratios assuming no decomposition were calculated for the mean ages of air, with the latter based on the measured age-of-air tracers. However, the actual mixing ratios measured in the samples were lower, indicating that there was decomposition of these ODSs and mixing with “older” air masses. We used the difference between the mixing ratios assuming no decomposition (given a particular mean age-of-air) and the measured mixing ratios in AMO-16 and AMA-17 to calculate the fraction of the ECI that had already been released for each compound. These measures are known as fractional release factors (FRFs). The more long-lived a compound is, the less decomposition takes place and the smaller their FRF is at the same mean age-of-air. Importantly, we used an improved method of FRF calculation (Ostermüller et al., 2017), which takes into account the dependency of the FRFs on the stratospheric lifetime of an ODS. The FRF uncertainties were calculated using the stratospheric measurement precisions, a proxy of the interhemispheric gradient in the troposphere, and the uncertainty in the tropospheric time series based on ground-based measurements.

For some of the FRF-mean-age correlations, the FRF was negative around mean ages of air of zero years. This was because our samples were collected above a polluted continental region so in some cases the mixing ratios of the remote tropospheric monitoring stations were lower than the mixing ratios observed in the ASMA tropopause region. This would cause our FRFs to have a low bias. Therefore, FRFs at a mean age-of-air of zero years were calculated from the respective FRF-mean age correlations (using a second order polynomial fit function) and when significantly different from zero, they were subtracted from the FRFs to calculate corrected FRFs. The FRFs of CFC-115, CFC-114a, HCFC-133a,  $\text{CH}_3\text{CCl}_3$ , Halon-1202,  $\text{CH}_3\text{Cl}$ , and  $\text{CH}_3\text{Br}$  were shifted in this way. This correction method relies on the assumption that the trace gases measured in 3-year-old air originated from a similarly polluted air mass below the tropopause, whereas it could in principal have come from somewhere else. The fact that we do observe continuity throughout the profile gives some confidence, but we note that this introduces an additional uncertainty to these FRFs, which we therefore refer to as regional FRFs. The FRFs in general agree with other FRFs calculated in the literature. For more information, see the supporting information material.

For the VSLs, it was not possible to use tropospheric trends at background stations to calculate FRFs because of significant loss and variability in the troposphere and the wide range of mixing ratios observed near the tropopause. Therefore, simplified FRFs were calculated by comparing the highest and lowest measured mixing ratios in the tropopause region (355–375 K) to the measured mixing ratios above 375 K in the campaigns.

For AMA-17, measurements of CFC-114, CFC-114a, CFC-13,  $\text{CH}_3\text{Cl}$ , Halon-1202, and  $\text{CCl}_4$  mixing ratios were only available for some of the samples. Therefore, the correlations of the available mixing ratios and FRFs with those of CFC-11 were used to estimate the values for the missing samples. Due to the set-up of

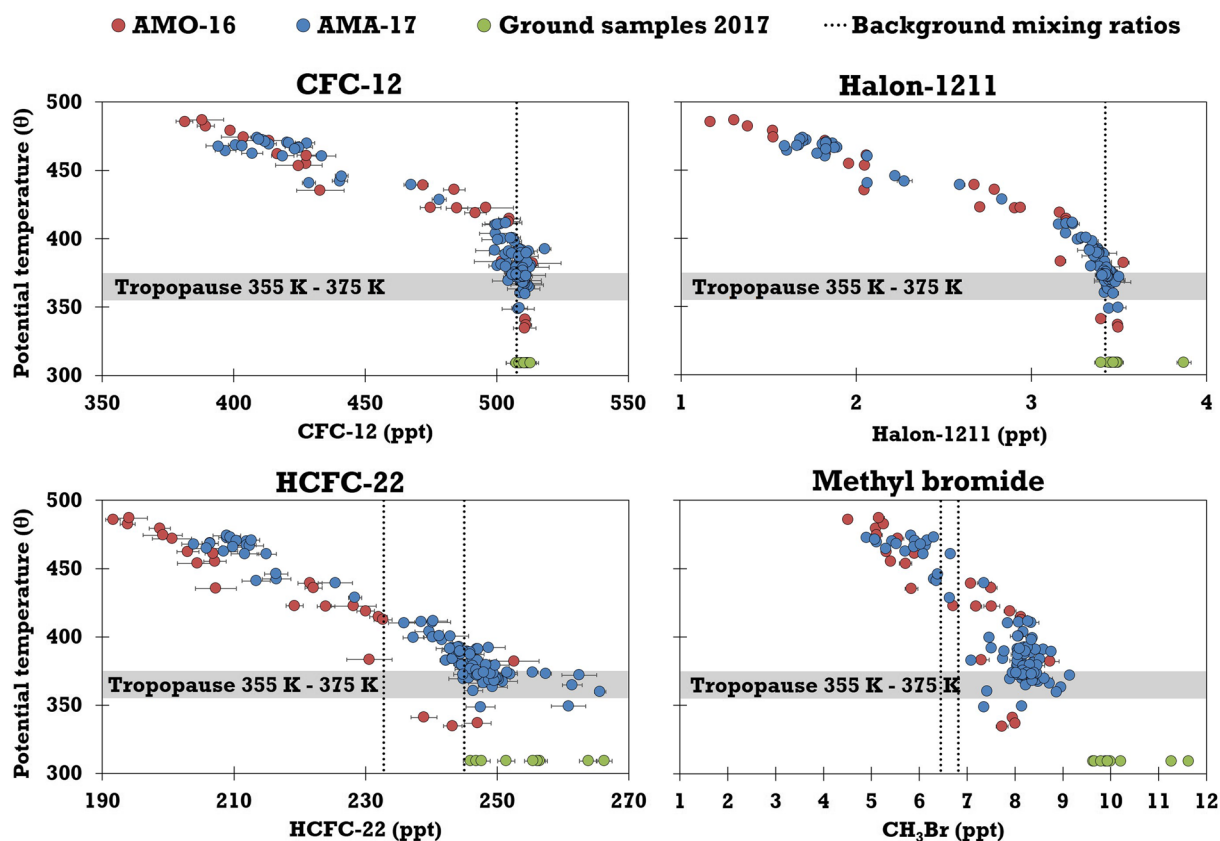


**Figure 2.** Mixing ratios of CFC-12, Halon-1211, HCFC-22, and methyl bromide ( $\text{CH}_3\text{Br}$ ) as a function of potential temperature (a pseudo-vertical coordinate) for AMO-16, AMA-17 and the ground samples collected during AMA-17. The dotted vertical line indicates the globally averaged background mixing ratios of CFC-12 and Halon-1211 for July–August 2017 from NOAA ground-based data (Table S1). Two background levels are indicated for HCFC-22 and  $\text{CH}_3\text{Br}$ , the lower one is from measurements at American Samoa ( $14.2^\circ\text{S}$ ,  $170.6^\circ\text{W}$ ) and the higher one from Mauna Loa ( $19.5^\circ\text{N}$ ,  $155.6^\circ\text{W}$ ; Table S1).

the instrument some compounds were not measured or exhibited poor quality and were therefore excluded from the EESC estimate:  $\text{CHClCCl}_2$ ,  $\text{CCl}_2\text{CCl}_2$ ,  $\text{CHBr}_3$ ,  $\text{CH}_2\text{BrCl}$ ,  $\text{CHBr}_2\text{Cl}$ ,  $\text{CHBrCl}_2$ , CFC-112, CFC-112a, HCFC-124, and Halon-2402.

To summarize, EESC depends on three factors: the mixing ratios of ODSs in the troposphere, the transport from the troposphere to the stratosphere (mean age-of-air) and breakdown of ODSs in the stratosphere (FRFs). The EESC was calculated and compared to other estimates in the literature in order to assess the overall impact on stratospheric ozone from ODSs in both campaigns.

### 3. Results and Discussion

#### 3.1. Long-Lived ODSs

CFC-12 and Halon-1211 in Figure 2 illustrates the observed distributions of long-lived ODSs that have been phased out under the Montreal Protocol. These two gases have only relatively small emission sources to the atmosphere in the monsoon input region and therefore their mixing ratios in the tropopause are not very variable. The ground-based AMA-17 samples and the lower aircraft measurements generally agree with the expected low variability as well as the NOAA background mixing ratios (Figure 2, top). This pattern is similar to what is found for many other long-lived ODSs in this study (see supporting information). Conversely, HCFC-22 and  $\text{CH}_3\text{Br}$  are significantly enhanced above expected background mixing ratios, on average by 5% for HCFC-22 and 25% for  $\text{CH}_3\text{Br}$  (Figure 2, bottom). Enhancements are also observed for HCFC-141b (6%) and  $\text{CH}_3\text{Cl}$  (14%; see supporting information). These enhancements indicate continued large emissions of these compounds in the monsoon input region.

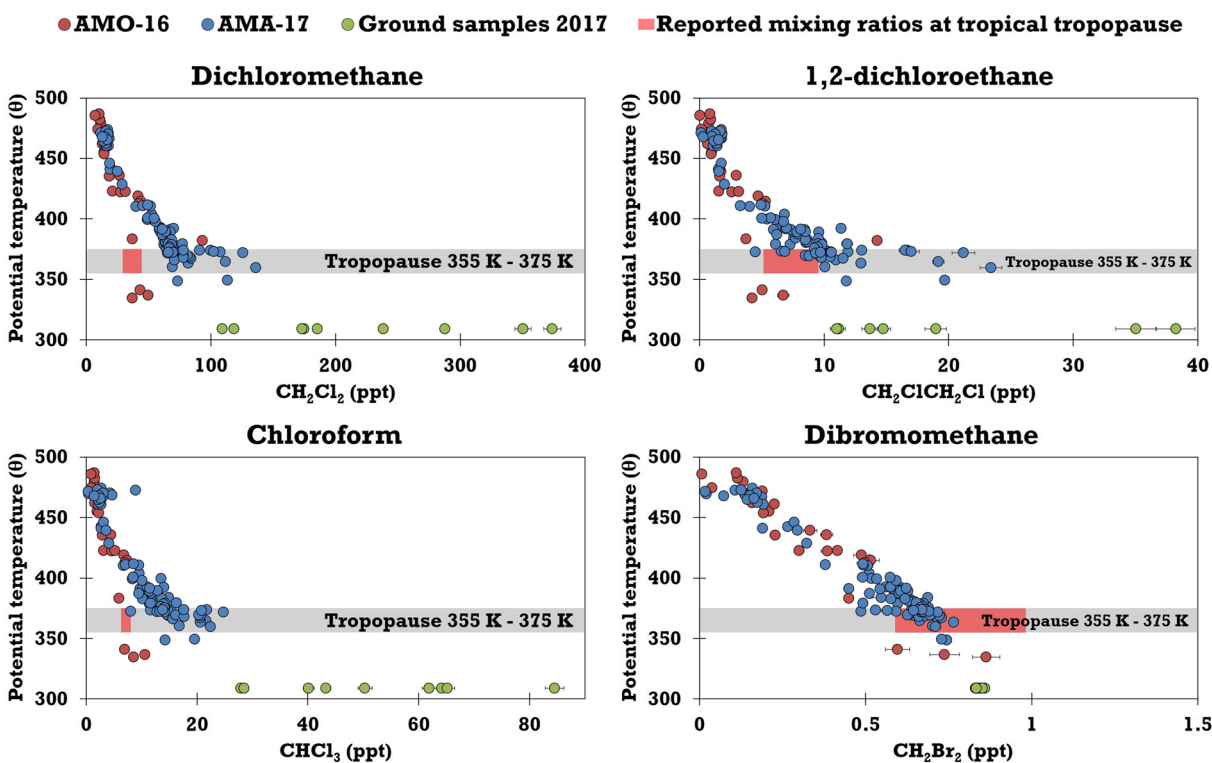


**Figure 3.** Mixing ratios for dichloromethane, 1,2-dichloroethane, chloroform, and dibromomethane ( $\text{CH}_2\text{Br}_2$ ) as a function of potential temperature for AMO-16, AMA-17, and the AMA-17 ground samples. The red shaded region indicates the estimated mixing ratios at the level of zero radiative heating (LZRH) for 2013–2014 from the WMO 2018 report (Engel, Rigby et al., 2018b; Table S1).

Among long-lived gases, Halon-1211 has a relatively short atmospheric lifetime of about 16 years. Halon-1211 mixing ratios in the tropopause region are similar to mixing ratios at the surface and NOAA ground-based mixing ratios indicating relatively little photolytic destruction of Halon-1211 in the troposphere in the ASMA region, as expected (Figure 2). At higher potential temperatures and therefore altitudes, in the stratosphere, the mixing ratios decrease due to photochemical degradation and mixing with other stratospheric air masses (Figure 2). Halon-1211 has a similar vertical profile to CFC-11, which also begins to decrease around the same potential temperature (see supporting information). The beginning of the decrease of Halon-1211 and CFC-11 mixing ratios therefore indicates that air has entered the lower stratosphere and constrains the location of the chemical tropopause. Other data (Brunamonti et al., 2018; Vogel et al., 2019) indicate that there is a transition region between the troposphere and the stratosphere at the top of the anticyclone. For our purposes using the ODS-based one is most appropriate as we are looking at similar gases. In this study, we define the location of the chemical transition layer between the troposphere and stratosphere to be the region of 355–375 K (i.e., just below the level at which Halon-1211 starts to decrease) which is represented by the horizontal gray bar in Figure 2. The location of the tropopause region is important because of the slow ascent rates representing a transport barrier that limits particularly the contribution of VSLs (due to their quicker chemical decomposition) to ozone depletion in the stratosphere.

### 3.2. Very Short-Lived Substances

The mixing ratios of the three major chlorinated VSLs,  $\text{CH}_2\text{Cl}_2$ ,  $\text{CH}_2\text{ClCH}_2\text{Cl}$ , and  $\text{CHCl}_3$ , and one brominated VSL, dibromomethane ( $\text{CH}_2\text{Br}_2$ ) are shown in Figure 3 as a function of potential temperature. The chlorinated VSLs show a large range of mixing ratios both in the ground-based samples (similar to many regions in Asia, e.g., Fang et al., 2019; Oram et al., 2017) and in the tropopause region indicating continued large emissions, which reach the tropopause (Figure 3). At higher potential temperatures, their mixing



**Table 1**  
*Comparison of the Global Estimate of Equivalent Chlorine (ECl) Based on Cape Grim, NOAA and WMO Mixing Ratios (See S1) and the Regional Estimate Based on the Air Samples From AMA-17*

	Global estimate ECl (ppt) 355–365 K	AMA-17 ECl (ppt) 355–375 K
<b>Chlorinated VSLs</b>	<b>89–132 (2%–3%)</b>	<b>163–393 (4%–8%)</b>
CH <sub>2</sub> Cl <sub>2</sub>	59–89	130–272
CHCl <sub>3</sub>	19–24	24–74
CH <sub>2</sub> ClCH <sub>2</sub> Cl	10–19	9–47
<b>Brominated VSLs</b>	<b>71–118</b>	<b>58–92</b>
CH <sub>2</sub> Br <sub>2</sub>	71–118	58–92
<b>Long-lived chlorine</b>	<b>3,159–3,186</b>	<b>3,188–3,356</b>
CFCs	1,960	1,939–1,997
HCFCs	310	317–343
CH <sub>3</sub> CCl <sub>3</sub>	6.5	4.8–6.0
CCl <sub>4</sub>	321	321–338
CH <sub>3</sub> Cl	558–586	603–669
Halon-1211	3.4	3.4–3.5
<b>Long-lived bromine</b>	<b>789–811</b>	<b>842–963</b>
Halons	402	398–414
CH <sub>3</sub> Br	387–409	445–549
<b>Estimated (not measured)<sup>a</sup></b>	<b>79–253</b>	<b>79–253</b>
<b>Total equivalent chlorine (ECl)</b>	<b>4,186–4,499</b>	<b>4,331–5,057</b>
	<b>(4,107–4,246)<sup>b</sup></b>	<b>(4,252–4,804)<sup>b</sup></b>

Abbreviation: VSLs, very short-lived substance.

<sup>a</sup>For the compounds that were not measured in this study the WMO 2018 reported values were used in both estimates.

<sup>b</sup>ECl excluding compounds that were not measured in this study.

ratios decrease rapidly as in the stratosphere they are broken down, predominantly by hydroxyl radical oxidation (Figure 3).

From WMO 2018 (Engel, Rigby et al., 2018b), estimated mixing ratios of these compounds in the tropical tropopause region (as derived from multiple aircraft campaigns in 2013–2014) are represented by the red-shaded areas indicated at the tropopause levels (Table S1 and Figure 3). The chlorinated VSLs in the tropopause region during AMA-17 are enhanced above the results from measurements in the tropical tropopause layer in 2013–2014 (Engel, Rigby et al., 2018b) on average by 124% for CH<sub>2</sub>Cl<sub>2</sub>, by 76% for CH<sub>2</sub>ClCH<sub>2</sub>Cl, and by 136% for CHCl<sub>3</sub>. Chlorine loading in the tropopause region from these three VSLs is 169–393 ppt in AMA-17 compared to the 89–132 ppt stated in the WMO 2018 report (Table 1). The global mean CH<sub>2</sub>Cl<sub>2</sub> mixing ratio measured at NOAA increased by about 10% from 2013–2014 to 2017, but this increase is not large enough to explain the difference. The mixing ratios are still enhanced above these data presented in WMO 2018 until about 400 K potential temperature. These estimates are for two different stratospheric entry points. The estimates in this study are for the ASMA tropopause region where there is a collocation of efficient vertical lifting from Earth's boundary layer to UTLS altitudes, with surface industrial emissions of chlorinated VSLs in Asian countries. Whereas, the WMO 2018 estimates are largely based on measurements from the tropical tropopause region, which is also influenced by strong convection but likely represents an average of regions with smaller underlying surface emissions of chlorinated VSLs than the ASMA region. CH<sub>2</sub>Br<sub>2</sub>, in contrast to the three chlorinated VSLs, has mostly natural oceanic sources, and its mixing ratios measured near the tropopause agree within the range of these data presented in WMO 2018 (Figure 3).

Samples collected during AMO-16 often have lower mixing ratios for the chlorinated VSLs than the samples from AMA-17 in the aircraft measurements at lower levels of potential temperature. This is possibly

because during AMO-16 in general two different types of air masses were sampled: mid-latitude extratropical air with lower mixing ratios and monsoon outflow-influenced air with higher mixing ratios, but not necessarily Asian sources.

Mixing ratios of these three chlorinated VSLs are well correlated, even in the more source-influenced upper tropospheric region. For AMA-17, the three aircraft samples with the highest  $\text{CH}_2\text{Cl}_2$  mixing ratios are also the samples with the three highest  $\text{CH}_2\text{ClCH}_2\text{Cl}$  and  $\text{CHCl}_3$  mixing ratios. For AMO-16, the sample with the highest  $\text{CH}_2\text{Cl}_2$  mixing ratio also has the highest  $\text{CH}_2\text{ClCH}_2\text{Cl}$  and  $\text{CHCl}_3$  mixing ratios. There is one outlier in AMA-17 which has high  $\text{CH}_2\text{Cl}_2$  mixing ratios but is not particularly enhanced for the other compounds ( $\text{CH}_2\text{Cl}_2$  107 ppt, 305 K, see supporting information). This suggests that the enhanced  $\text{CH}_2\text{Cl}_2$  in this sample originates from a different source. In addition, an influence from the tropospheric trends could play a role in these correlations as both  $\text{CHCl}_3$  and  $\text{CH}_2\text{Cl}_2$  have been increasing in recent years (Engel, Rigby et al., 2018b). Given that the samples with high mixing ratios of these three chlorinated VSLs are all at low altitudes and contain relatively young air this influence can however be neglected here.

In addition to having strong correlations with each other, the chlorinated VSLs are also correlated with other compounds. When investigating only the samples in the tropopause region using Spearman correlations (i.e., assuming a monotonic but not necessarily linear relationship) and excluding the outlier sample,  $\text{CH}_2\text{Cl}_2$  has the strongest Spearman's correlation coefficients with  $\text{CHCl}_3$  ( $R = 0.87$ ), HFC-32 ( $R = 0.87$ ), HCFC-22 ( $R = 0.87$ ),  $\text{CH}_2\text{ClCH}_2\text{Cl}$  ( $R = 0.75$ ), and HFC-125 ( $R = 0.74$ ).  $\text{CH}_2\text{ClCH}_2\text{Cl}$  has the strongest positive Spearman's correlations with  $\text{CH}_2\text{Cl}_2$  ( $R = 0.75$ ), HCFC-133a ( $R = 0.71$ ),  $\text{CHCl}_3$  ( $R = 0.70$ ),  $\text{CCl}_4$  ( $R = 0.66$ ), and HFC-23 ( $R = 0.66$ ). The compounds that are well correlated with  $\text{CHCl}_3$  are  $\text{CH}_2\text{Cl}_2$  ( $R = 0.87$ ), HFC-32 ( $R = 0.82$ ), HFC-125 ( $R = 0.72$ ),  $\text{SF}_6$  ( $R = 0.71$ ), and  $\text{CH}_2\text{ClCH}_2\text{Cl}$  ( $R = 0.70$ ; see supporting information). These correlations are all significant ( $p < 0.01$ ) and all of the compounds have known strong industrial emissions in East and South-East Asia (Fang et al., 2019, 2018; Kim et al., 2010; Lunt et al., 2018; Vollmer et al., 2015); suggesting the sources of the halogenated compounds in these air samples are from continental industrial areas and indicating that they are either emitted from colocated sources or coproduced. The strongest correlation is between  $\text{CH}_2\text{Cl}_2$  and  $\text{CHCl}_3$  and these two compounds are known to be coproduced in large quantities in East Asia (Oram et al., 2017).

### 3.3. CLaMS Backward Trajectory Calculations

The possible source regions in the Earth's model boundary layer of  $\text{CH}_2\text{Cl}_2$  in the AMA-17 air samples were investigated using 10-day CLaMS backward trajectories driven by ERA5. Figure 4 shows the end points of the 10-day backward trajectories, the location where the air was last in the model boundary layer, that is, 2–3 km above the surface. It should be noted that of all the 10-day backward trajectories calculated, only 9% of them have end points in the model boundary layer; the rest of the trajectories end in the free troposphere and stratosphere. Therefore, the trajectory end points reflect only the contributions of the very young air masses (<10 days) to the composition of the air samples.

Our analysis shows that clusters of trajectory end points in the model boundary layer exist that correspond to air samples with high  $\text{CH}_2\text{Cl}_2$  mixing ratios (red colors) located in east Asia (mainly in China) and at the north-western flank of the Tibetan Plateau (Northwest India and North Pakistan) and for a trajectory length of 15 days also in Northern India (not shown here). Red points are only found if  $\text{CH}_2\text{Cl}_2$ -polluted air masses in the lower troposphere experienced strong vertical uplift by convection. Therefore, the location of red points indicates possible source regions in South Asia with enhanced  $\text{CH}_2\text{Cl}_2$  emissions. Many of the possible source regions of high  $\text{CH}_2\text{Cl}_2$  mixing ratios found in our trajectory calculations are in China which is in agreement with sources of anthropogenic  $\text{CH}_2\text{Cl}_2$  emissions in Asia (e.g., Feng et al., 2018).

Clusters of trajectory end points in the model boundary layer with low  $\text{CH}_2\text{Cl}_2$  mixing ratios (blue colors) are mainly found in the region of the Tibetan Plateau, in the Bay of Bengal and in surrounding continental area, indicating the absence of significant anthropogenic  $\text{CH}_2\text{Cl}_2$  sources in these regions. For a trajectory length of 15 days, sources of low  $\text{CH}_2\text{Cl}_2$  mixing ratios are also found in Southeast Asia and over the Western Pacific (not shown here). In general, the longer the trajectories the wider the trajectory endpoints are distributed over South Asia caused by the trajectory dispersion depending on the trajectory length.

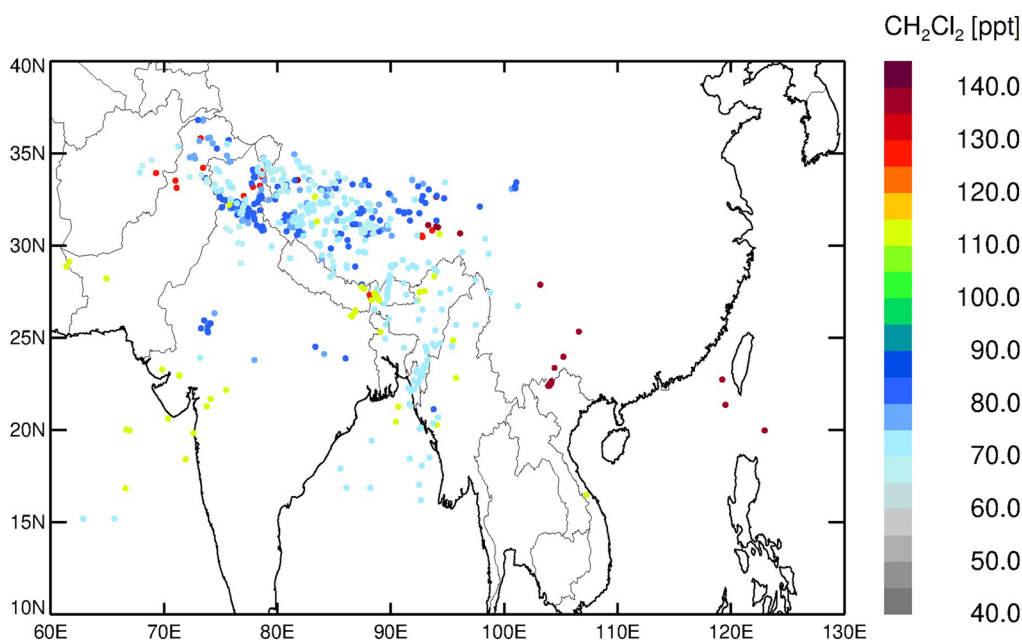


**Figure 4.** Location of end points of the CLaMS 10-day backward trajectories, initialized for each air sample (with 1-s resolution). Shown are only trajectory end points for air samples collected below 390 K potential temperature during AMA-17, where the trajectory reaches the model boundary layer (i.e., 2–3 km above the Earth’s surface following orography), within 10 days. The color of the data points indicates the  $\text{CH}_2\text{Cl}_2$  mixing ratios in the air sample collected at UTLS altitudes. CLaMS, Chemical Lagrangian Model of the Stratosphere; UTLS, upper troposphere and lower stratosphere.

### 3.4. Equivalent Chlorine

After analyzing the individual VSLs, their contribution to the total ECI in the tropopause region was investigated. Table 1 shows two estimates of ECI, one estimate derived using a similar methodology to that used in the WMO 2018 report (Engel, Rigby et al., 2018b) and the other estimate based on the air samples from AMA-17.

In the first method for calculating ECI, the tropospheric reference mixing ratios of the long-lived compounds were, as explained in Section 2.5, taken from NOAA (<https://www.esrl.noaa.gov/gmd/dv/ftpdata.html>). Similar to previous approaches (Laube, Engel et al., 2010b, Laube et al., 2013) either global mixing ratios were used, or in the case of compounds with significant tropospheric sinks such as HCFCs and methyl halides, data from the NOAA ground-based measurement sites at Mauna Loa (19.5°N, 155.6°W) and American Samoa (14.2°S, 170.6°W) in July–August 2017, the same time period as AMA-17, were used. As HCFCs and methyl halides have significant tropospheric sinks, using ground-based measurements can lead to a slight overestimation of their mixing ratios in the tropopause region. UEA measurements of air samples collected at Cape Grim, Tasmania, in early 2018 and shifted back in time by 6 months were used to complement this approach (see also Table S1). For the VSLs that are broken down rapidly in the troposphere and for which it is therefore much harder to estimate the proportion transported to the tropopause, the global estimates of tropospheric reference mixing ratios come from the WMO 2018 report for the level of zero radiative heating (LZRH; Engel, Rigby et al., 2018b). These mixing ratios of VSLs in the WMO 2018 report were based on results from the CAST (Coordinated Airborne Studies in the Tropics), CONTRAST (Convective Transport of Active Species in the Tropics), and ATTREX (Airborne Tropical Tropopause Experiment) aircraft campaigns that took place in the tropical West Pacific in 2013 and 2014 (Harris et al., 2017; Jensen et al., 2017; Pan et al., 2017). They were used to investigate the differences between the tropics and the ASMA input of VSLs in the lower stratosphere. It should be noted that mixing ratios of some of these compounds have changed over time and some of the reported values were on different calibration scales to the measurements in this study which may cause small differences.

There are some halogenated gases that were considered in Engel, Rigby et al. (2018b) but were not available from the AMA-17 samples:  $\text{CHClCCl}_2$ ,  $\text{CCl}_2\text{CCl}_2$ ,  $\text{CHBr}_3$ ,  $\text{CH}_2\text{BrCl}$ ,  $\text{CHBr}_2\text{Cl}$ ,  $\text{CHBrCl}_2$ , CFC-112, CFC-112a, HCFC-124, and Halon-2402. For these compounds, we used the same mixing ratios from the Engel, Rigby et al. (2018b) in both estimates to make them comparable. In total, these compounds contribute 79–253 ppt to ECl. See supporting information for more information.

For the global estimates of ECl, a potential temperature range of 355–365 K was used. This is the range of the tropical tropopause layer or the LZRH in the WMO 2018 report (Engel, Rigby et al., 2018b). Air at this altitude is likely to continue to ascend into the lower tropical stratosphere by radiative heating. Some studies have suggested that the LZRH may be pushed upwards by the ASMA as air from the troposphere rises, creating an elevated tropopause (e.g., Dethof et al., 1999; Dunkerton, 1995; Highwood & Hoskins, 1998; Ploeger et al., 2017). To take this into account, we used an increased potential temperature range of 355–375 K for estimates based on the AMA-17 air samples, which also agrees with our own observations of gases with exclusively stratospheric sinks such as Halon-1211 (Figure 2). There were 27 samples collected in this range during AMA-17 and these were used to estimate the ECl. An ECl estimate for AMO-16 was not calculated as no air samples were collected in the tropopause region in this campaign (and much fewer samples were collected in general). Note that we did not consider ECl contributions from the breakdown products of VSLs in this study, so our ECl can be considered a lower limit of the total chlorine and bromine entering the stratosphere via the ASMA.

Table 1 shows that the total ECl from the AMA-17 aircraft campaign is higher than the total ECl from the global estimates based on Cape Grim, NOAA and WMO mixing ratios. However, the AMA-17-based ECl also has a wider range and the lower end of the range overlaps with the higher end of the range for the global estimate (Table 1). So there is not a significant difference between the overall ECl range estimates. This is due to many of our samples in the tropopause having higher mixing ratios of ODSs than in the previous global estimates while some samples also show mixing ratios in the range of the global estimates (Sections 3.1 and 3.2).

The compounds contributing to the ECl were divided into four categories: chlorinated VSLs, brominated VSLs ( $\text{CH}_2\text{Br}_2$ ), long-lived chlorine and long-lived bromine (Table 1). Both estimates for  $\text{CH}_2\text{Br}_2$  have large ranges that overlap. The long-lived chlorine in the AMA-17 samples is slightly higher than the global estimate. This is because mixing ratios of the CFCs and carbon tetrachloride ( $\text{CCl}_4$ ) agree within our range, methyl chloroform ( $\text{CH}_3\text{CCl}_3$ ) is slightly smaller in the AMA-17 estimate, and HCFCs and methyl chloride ( $\text{CH}_3\text{Cl}$ ) are slightly larger. This is qualitatively in line with the findings of Umezawa et al. (2014) who found enhancements of  $\text{CH}_3\text{Cl}$  in the ASMA region at lower altitudes that may be related to biomass and biofuel emissions. For the long-lived bromine species, the AMA-17 estimate is also slightly higher than the global estimate. Here, the halon mixing ratios agree with the AMA-17 estimate, so the higher long-lived bromine estimate for AMA-17 is almost completely due to methyl bromide ( $\text{CH}_3\text{Br}$ ) (6.5–6.8 ppt vs. 7.4–9.1 ppt) indicating larger sources of methyl bromide in the monsoon input region.

Mixing ratios of chlorinated VSLs are higher in the AMA-17 estimate than in the estimate based on WMO 2018 mixing ratios at the LZRH. In the latter estimate chlorinated VSLs contribute about 2%–3% to the total ECl entering the stratosphere whereas in the AMA-17 estimate this is higher, 4%–8% of the total ECl. We note that the AMA-17 estimate is for a particular region and a particular time of year when there is likely to be a very high injection rate during the ASMA (Leedham Elvidge et al., 2015). The WMO 2018 values incorporate measurements from various campaigns and are more representative of the input from the tropics. In both estimates chlorinated VSLs make up a relatively small fraction of the total ECl in the tropopause region.

The influence of the ASMA on the stratosphere is largest in the Northern Hemisphere, there is a smaller influence on air in the tropical stratosphere and an even smaller influence on the stratosphere in the Southern Hemisphere (Ploeger et al., 2017; Yan et al., 2019). Using the results in Ploeger et al. (2017) we calculated that, averaged over the whole year, 5% of the air in the Northern Hemispheric lower stratosphere comes from the ASMA. If we assume that 5% of the additional ECl from the AMA-17 estimate ends up in the lower stratosphere of the Northern Hemisphere, this translates to an additional 0.3–34.9 ppt of ECl from all measured compounds, of which 1.6–15.2 ppt are from chlorinated VSLs. Total tropospheric chlorine from

controlled substances has been decreasing by  $12.7 \pm 0.92$  ppt Cl yr<sup>-1</sup> while that from uncontrolled substances (CH<sub>3</sub>Cl and chlorinated VSLs) has been increasing by  $8.3 \pm 4.9$  ppt Cl yr<sup>-1</sup>, leading to an overall decrease of  $4.4 \pm 4.1$  ppt Cl yr<sup>-1</sup> between 2012 and 2016 (Engel, Rigby et al., 2018b). The decrease in chlorine from controlled ODSs has been partially offset by the increase in CH<sub>3</sub>Cl and chlorinated VSLs (Engel, Rigby et al., 2018b). These current annual decreases are up to six times smaller than the additional 0.3–34.9 ppt we calculated from chlorinated VSLs. Although these elevated mixing ratios are only observed in one part of the atmosphere it indicates that the influence of the enhanced mixing ratios of the methyl halides as well as the chlorinated VSLs may be significant.

### 3.5. Equivalent Effective Stratospheric Chlorine

EESC was calculated for a mean age-of-air of 3 years for AMO-16 as this is the mean age-of-air usually used in the literature to approximate mid-latitude ozone depletion. EESC was also calculated for a mean age-of-air of 2.4 years for both campaigns in order to compare the campaigns. The EESC was calculated using tropospheric trends from the same NOAA and Cape Grim data sets mentioned above (Section 3.4), mixing ratios from the aircraft samples to calculate time-independent FRFs (see supporting information) and an adjusted mean age-of-air (see supporting information).

For both campaigns, EESC was calculated using the “relevant age EESC” method from Engel, Bönisch et al. (2018a). The “relevant age EESC” is a refinement in the calculation method of EESC. A previous method (Newman et al., 2007) was based on the assumption that the age spectrum for an inert species is representative of the age spectrum of a chemically reactive species. This is not the case as the average age-of-air for source gases that have been dissociated in the stratosphere is longer than the average age of inert tracers in the same stratospheric location (Engel, Bönisch et al., 2018a; Plumb et al., 1999). Younger air contains more reactive species than older air so the organic fraction of a chemically active species is largely determined by the fraction of the air with shorter transit times (Plumb et al., 1999). To take into account the interaction between chemical loss and transit time, the relevant age EESC method uses new time-independent FRFs (Ostermüller et al., 2017) and an age spectrum weighted by chemical loss (Engel, Bönisch et al., 2018a). The EESC was also calculated based on the older mean-age based method (Newman et al., 2007). This gives similar results with a quantitative comparison being available in supporting information.

In addition, each estimate has a range because of the relatively short lifetime of CH<sub>3</sub>Br and CH<sub>3</sub>Cl. The EESC contribution of these two compounds was calculated twice: using again tropospheric trends from Mauna Loa and American Samoa. The lower end of the range is based on Mauna Loa trends and the higher end of the range is based on American Samoa trends. Neither of these sites are ideal for estimates of the amount of shorter-lived ODSs reaching the tropical upper troposphere, but they are the closest ground-based approximations available and yield similar FRFs (see supporting information).

The EESCs from this study were calculated using the same method used in Engel, Bönisch et al. (2018a). However, there are some differences between our EESCs and the Engel, Bönisch et al. (2018a) estimates:

1. The shifting of FRFs explained in Section 2.5 means that for some species the mixing ratios observed near the tropopause were significantly lower (CFC-115, CH<sub>3</sub>CCl<sub>3</sub>) or higher (CFC-114a, HCFC-133a, Halon-1202, CH<sub>3</sub>Cl, CH<sub>3</sub>Br) than expected from surface-based trends. This is likely due to the special nature of this region and season. The adjusted FRFs compare well with those from other studies in line with the expectation that they are dominated by common sinks and global tropospheric trends. It does however not take into account that the actual amount found near the tropopause is different, which is important for deriving a regional EESC. The difference was therefore calculated and added to all our regional EESC estimates
2. We included some minor compounds that Engel, Bönisch et al. (2018a) did not include (CFC-113a, HCFC-133a, and CFC-13). They also did not include CFC-114a but their CFC-114 mixing ratio is a combination of CFC-114 and CFC-114a
3. They included Halon-2402 and due to small contamination problems, this was not possible here

Therefore, to compare our EESC to Engel, Bönisch et al. (2018a), we recalculated our EESC excluding CFC-113a, HCFC-133a, and CFC-13. Including these species makes very little difference, it adds only ~1 ppt to



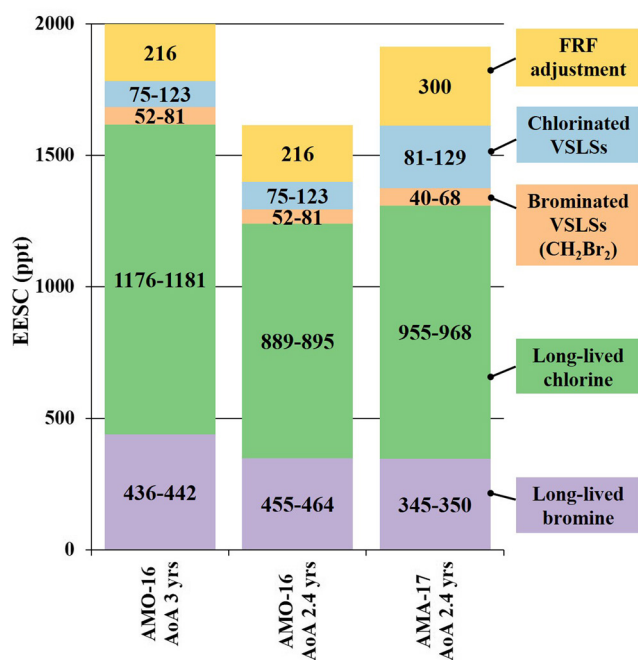


**Figure 5.** EESC at mean age-of-air of 2.4 years for the AMO-16 and AMA-17 campaigns and at mean age-of-air of 3 years for the AMO-16 campaign, calculated using relevant age and mean age, showing the contributions from long-lived and very short-lived chlorine and bromine. AoA, age-of-air; EESC, equivalent effective stratospheric chlorine.

the EESCs, well within the uncertainty of the estimate. We determined the contribution of Halon-2402 to our EESC estimates using the 2017 mean tropospheric mixing ratio and the FRF given in Engel, Bönisch et al. (2018a), to arrive at an additional contribution of ~33 ppt from this molecule.

For AMO-16 the EESC is 12% higher (1,861–1,872 ppt) than the Engel, Bönisch et al. (2018a) estimate for an age-of-air of 3 years (1,646 ppt). At an age-of-air of 2.4 years EESC is lower in AMO-16 than in AMA-17 by about 135 ppt. This is likely because during AMO-16 different types of air masses were sampled: outflow from the Asian monsoon and Northern Hemispheric extratropical air. It implies that, if it was measured, the EESC above the ASMA at an age-of-air of 3 years may be much higher than the Engel, Bönisch et al. (2018a) EESC estimate.

To investigate the impact of VSLs on lower stratospheric ozone depletion, an EESC contribution for these substances was calculated. The EESC contribution at 2.4 years mean age-of-air from our VSLs is between 121 and 197 ppt based on the air samples collected during AMO-16 and 174–437 ppt based on the air samples collected during AMA-17 (Figure 5). This is about 8%–26% of the EESC from long-lived compounds (Figure 5). This inclusion increases both the EESC and its range (Table 2) and indicates that the contribution of VSLs is relatively larger in the northern hemispheric lower stratosphere where there is less fractional release of reactive chlorine from the longer-lived species. Moreover, the total EESC contribution from these VSLs may be higher than our estimate as some fraction of the halogenated “product gases” from their tropospheric breakdown may also be injected in to the stratosphere (“product gas injection” is discussed in Engel, Rigby et al., 2018b). There are also

other VSLs not measured in this study that may contribute (e.g., CHBr<sub>3</sub>, CH<sub>3</sub>(CH<sub>2</sub>)<sub>2</sub>Br, and other anthropogenic chlorocarbons).

Assuming a linear trend, EESC at mid-latitudes has decreased by 14–16 ppt per year from its peak values to 2017 (Engel, Rigby et al., 2018b). This gives some context to the size of the contribution from VSLs observed in measurements from both campaigns compared to the size of the decreasing trend.

#### 4. Conclusions

Air samples collected in the UTLS on board the high-altitude Geophysica research aircraft in the vicinity of and within the ASMA were found to have substantially elevated mixing ratios of chlorinated VSLs compared to WMO 2018 estimates (Engel, Rigby et al., 2018b). For example, CH<sub>2</sub>Cl<sub>2</sub> mixing ratios were 30–44 ppt in the tropical tropopause region in 2013–2014, as stated in the WMO 2018 report, but 65–136 ppt in the ASMA tropopause region in 2017, based on the AMA-17 samples. This is likely largely due to the rapid transport of emissions of these substances from South Asia to the UTLS via the ASMA and higher-than-global emission rates in this region. We show that VSLs are transported irreversibly from the ASMA into the lower stratosphere where they will contribute to ozone depletion. The contribution of chlorinated VSLs is significantly higher in this region than that reported in the WMO Scientific Assessment of Ozone Depletion (Engel, Rigby et al., 2018b) in terms of ECI in the tropopause region (89–132 ppt vs. 169–393 ppt). These additional VSL contributions increase the estimate of EESC in the Northern Hemisphere extratropical lower stratosphere by 8%–26%.

Our estimates of ECI and EESC from long-lived species in the stratosphere in this region are generally larger than global average values based on Engel, Bönisch et al. (2018a). For example, EESC at 3 years in Engel, Bönisch et al. (2018a) is 1,646 ppt, whereas the AMO-16-based range is 1,861–1,872 ppt. ECI from long-lived species is 3,947–3,997 ppt in the global estimate and 4,031–4,319 ppt in the AMA-17 estimate. The ASMA region generally has large continental emissions and more input into the stratosphere than many

**Table 2**  
*Regional Equivalent Effective Stratospheric Chlorine (EESC) Estimates From the AMO-16 and AMA-17 Campaigns Calculated Using the Relevant age*

Campaign	EESC <sup>a</sup>	EESC + VSLs <sup>b</sup>
AMA-17 (age-of-air 2.4 years)	1,630–1,650	1,804–2,087
AMO-16 (age-of-air 2.4 years)	1,483–1,495	1,604–1,692
AMO-16 (age-of-air 3 years)	1,861–1,872	1,988–2,075
Engel, Bönisch et al. (2018a) (age-of-air 3 years)	1,646 (in 2017)	–

Note. Also shown is the global EESC estimate from Engel, Bönisch et al. (2018b).

<sup>a</sup>EESC including CFC-13, CFC-113a, HCFC-133a, and Halon-2402. <sup>b</sup>EESC<sup>a</sup> with an additional contribution from very short-lived substances (VSLs).

other regions. This explains why the AMA-17 estimate is larger than the global average from WMO as it is impacted by regional emissions to a larger degree than global mean estimates.

A previous study found similar enhanced mixing ratios of CH<sub>2</sub>Cl<sub>2</sub>, CH<sub>2</sub>ClCH<sub>2</sub>Cl, and CHCl<sub>3</sub> in the upper tropopause region during boreal winter over South-East Asia, indicating that rapid upward transport also occurs in the winter monsoon (Oram et al., 2017). The additional input of chlorine into the stratosphere from these sources could delay the recovery of the ozone layer if the growth rate of chlorinated VSLs persists in the future (Hossaini et al., 2017). Since our observations are both spatially and temporally limited the quantification of this possible future impact is beyond the scope of this study.

However, when combining the differences between the most recent WMO ECl estimates (Engel, Rigby et al., 2018b) and our AMA-17-based ECl (Table 1) with the estimate from Ploeger et al. (2017) of the monsoon contributing an annual average of about 5% to Northern Hemispheric lower stratospheric air, we derive a difference ranging from 0.3–34.9 ppt of ECl from all measured compounds, much of it in the form of chlorinated VSLs. Depending on the interannual monsoon variability as well as how much ECl enters this part of the stratosphere via the tropical West Pacific and through extratropical isentropic transport, the available levels of chlorine and bromine might thus be substantially higher than the global average derived from global ground-based measurements. In summary, this work highlights the importance of both the ASMA as a fast transport mechanism in an important ODS emission region, and the role of chlorinated VSLs for stratospheric ozone, particularly in the northern extratropical lower stratosphere during the Northern Hemisphere summer and autumn.

### Author Contributions

Karina Adcock wrote the article and did most of the data analysis. Bärbel Vogel produced the output from the CLaMS chemistry-transport model, which Karina Adcock then compared to the atmospheric observations. Geoffrey Lee, Johannes Laube, and Karina Adcock measured and analyzed the air samples used in this study. In addition, Johannes Laube and Karina Adcock worked together to calculate the fractional release factors, Equivalent Chlorine and Equivalent Effective Stratospheric Chlorine. Johannes Laube and William Sturges coordinated activities for the University of East Anglia (UEA) related to the StratoClim aircraft campaigns. Paul Fraser, Ray Langenfelds and David Oram organized the collection of samples from the Cape Grim Monitoring Station. Bradley Hall and Stephen Montzka were involved in producing the NOAA atmospheric observations that were used in this study. Fred Stroh coordinated the aircraft campaigns while Thomas Röckmann coordinated the operation a whole air sampler on the research aircraft to collect the air samples used in this study. In addition, all of the co-authors contributed comments and suggestions for editing this work.

### Data Availability Statement

The data are available from the Zenodo repository, doi:10.5281/zenodo.3836630.

**Acknowledgments**

We are grateful for the contributions of Michel Bolder, Carina van der Veen (both Utrecht University), and the Geophysica team (sample collection and campaign organization), Guus Velders and Andreas Engel (EESC comparisons), Elinor Tuffnell (data processing) and the NOAA Global Monitoring Division (surface halocarbon data). We thank the staff at the Cape Grim station and at CSIRO GASLAB Aspendale for collecting and maintaining the Cape Grim air archive and preparing the UEA flasks and sub-samples. We also acknowledge CSIRO and the Bureau of Meteorology for funding these activities. The StratoClim flights were funded by the European Commission (FP7 project Stratoclim-603557, [www.stratoclim.org](http://www.stratoclim.org)). This work was supported by the Natural Environment Research Council through the EnvEast Doctoral Training Partnership (grant number NE/L002582/1) as well as the ERC project EXC<sup>3</sup>ITE (EXC3ITE-678904-ERC-2015-STG). Johannes C. Laube received funding from the UK Natural Environment Research Council (Research Fellowship NE/1021918/1).

**References**

Andrews, A. E., Boering, K. A., Daube, B. C., Wofsy, S. C., Loewenstein, M., Jost, H., et al. (2001). Mean ages of stratospheric air derived from in situ observations of CO<sub>2</sub>, CH<sub>4</sub>, and N<sub>2</sub>O. *Journal of Geophysical Research*, 106(D23), 32295–32314. <https://doi.org/10.1029/2001JD000465>

Annamalai, H., & Slingo, J. M. (2001). Active/break cycles: Diagnosis of the intraseasonal variability of the Asian Summer Monsoon. *Climate Dynamics*, 18(1–2), 85–102. <https://doi.org/10.1007/s003820100161>

Ball, W. T., Alsing, J., Mortlock, D. J., Staehelin, J., Haigh, J. D., Peter, T., et al. (2018). Evidence for a continuous decline in lower stratospheric ozone offsetting ozone layer recovery. *Atmospheric Chemistry and Physics*, 18(2), 1379–1394. <https://doi.org/10.5194/acp-18-1379-2018>

Brioude, J., Portmann, R. W., Daniel, J. S., Cooper, O. R., Frost, G. J., Rosenlof, K. H., et al. (2010). Variations in ozone depletion potentials of very short-lived substances with season and emission region. *Geophysical Research Letters*, 37(19), 3–7. <https://doi.org/10.1029/2010GL044856>

Brunamonti, S., Jorge, T., Oelsner, P., Hanumanthu, S., Singh, B. B., Kumar, K. R., et al. (2018). Balloon-borne measurements of temperature, water vapor, ozone and aerosol backscatter at the southern slopes of the Himalayas during StratoClim 2016–2017. *Atmospheric Chemistry and Physics*, 18(21), 15937–15957. <https://doi.org/10.5194/acp-18-15937-2018>

Cairo, F., Pommereau, J. P., Law, K. S., Schlager, H., Garnier, A., Fierli, F., et al. (2010). An introduction to the SCOUT-AMMA stratospheric aircraft, balloons and sondes campaign in West Africa, August 2006: Rationale and roadmap. *Atmospheric Chemistry and Physics*, 10(5), 2237–2256. <https://doi.org/10.5194/acp-10-2237-2010>

Chipperfield, M. P., Dhomse, S., Hossaini, R., Feng, W., Santee, M. L., Weber, M., et al. (2018). On the cause of recent variations in lower stratospheric ozone. *Geophysical Research Letters*, 45(11), 5718–5726. <https://doi.org/10.1029/2018GL078071>

Claxton, T., Hossaini, R., Wilson, C., Montzka, S. A., Chipperfield, M. P., Wild, O., et al. (2020). A synthesis inversion to constrain global emissions of two very short lived chlorocarbons: Dichloromethane, and perchloroethylene. *Journal of Geophysical Research: Atmospheres*, 125(12), e2019JD031818. <https://doi.org/10.1029/2019JD031818>

Daniel, J. S., Velders, G. J. M., Douglass, A. R., Forster, P. M. D., Hauglustaine, D. A., Isaksen, I. S. A., et al. (2007). Halocarbon scenarios, ozone depletion potentials, and global warming potentials. In *Scientific assessment of ozone depletion: 2006 (Global Ozone Research and Monitoring Project-Rep. No. 50)*. Geneva, Switzerland: World Meteorological Organization.

Dee, D. P., Uppala, S. M., Simmons, A. J., Berrisford, P., Poli, P., Kobayashi, S., et al. (2011). The ERA-Interim reanalysis: Configuration and performance of the data assimilation system. *Quarterly Journal of the Royal Meteorological Society*, 137(656), 553–597. <https://doi.org/10.1002/qj.828>

Dethof, A., O’neill, A., Slingo, J. M., & Smit, H. G. J. (1999). A mechanism for moistening the lower stratosphere involving the Asian summer monsoon. *Quarterly Journal of the Royal Meteorological Society*, 125(556), 1079–1106. <https://doi.org/10.1002/qj.1999.49712555602>

Dunkerton, T. J. (1995). Evidence of meridional motion in the summer lower stratosphere adjacent to monsoon regions. *Journal of Geophysical Research*, 100(D8), 16675–16688. <https://doi.org/10.1029/95JD01263>

Engel, A., Bönisch, H., Ostermüller, J., Chipperfield, M. P., Dhomse, S., & Jöckel, P. (2018a). A refined method for calculating equivalent effective stratospheric chlorine. *Atmospheric Chemistry and Physics*, 18(2), 601–619. <https://doi.org/10.5194/acp-18-601-2018>

Engel, A., Rigby, M., Burkholder, J. B., Fernandez, R. P., Froidevaux, L., Hall, B. D., et al. (2018b). Update on ozone-depleting substances (ODSs) and other gases of interest to the Montreal Protocol. In *Scientific assessment of ozone depletion: 2018 (Global Ozone Research and Monitoring Project-Rep. No. 58)*. Geneva, Switzerland: World Meteorological Organization.

Engel, A., Strunk, M., Müller, M., Haase, H., Poss, C., Levin, I., & Schmidt, U. (2002). Temporal development of total chlorine in the high-latitude stratosphere based on reference distributions of mean age derived from CO<sub>2</sub> and SF<sub>6</sub>. *Journal of Geophysical Research*, 107(D12), ACH 1-1–ACH 1-11. <https://doi.org/10.1029/2001JD000584>

Fang, X., Park, S., Saito, T., Tunnicliffe, R., Ganesan, A. L., Rigby, M., et al. (2019). Rapid increase in ozone-depleting chloroform emissions from China. *Nature Geoscience*, 12(2), 89–93. <https://doi.org/10.1038/s41561-018-0278-2>

Fang, X., Ravishankara, A. R., Velders, G. J. M., Molina, M. J., Su, S., Zhang, J., et al. (2018). Changes in emissions of ozone-depleting substances from China due to implementation of the Montreal Protocol. *Environmental Science & Technology*, 52(19), 11359–11366. <https://doi.org/10.1021/acs.est.8b01280>

Feng, Y., Bie, P., Wang, Z., Wang, L., & Zhang, J. (2018). Bottom-up anthropogenic dichloromethane emission estimates from China for the period 2005–2016 and predictions of future emissions. *Atmospheric Environment*, 186, 241–247. <https://doi.org/10.1016/j.atmosenv.2018.05.039>

Garny, H., & Randel, W. J. (2013). Dynamic variability of the Asian monsoon anticyclone observed in potential vorticity and correlations with tracer distributions. *Journal of Geophysical Research: Atmospheres*, 118(24), 13421–13433. <https://doi.org/10.1002/2013JD020908>

Garny, H., & Randel, W. J. (2016). Transport pathways from the Asian monsoon anticyclone to the stratosphere. *Atmospheric Chemistry and Physics*, 16, 2703–2718. <https://doi.org/10.5194/acp-16-2703-2016>

Harris, N. R. P., Carpenter, L. J., Lee, J. D., Vaughan, G., Filus, M. T., Jones, R. L., et al. (2017). Coordinated airborne studies in the tropics (CAST). *Bulletin of the American Meteorological Society*, 98(1), 145–162. <https://doi.org/10.1175/BAMS-D-14-00290.1>

Harrison, J. J., Chipperfield, M. P., Hossaini, R., Boone, C. D., Dhomse, S., Feng, W., & Bernath, P. F. (2019). Phosgene in the upper troposphere and lower stratosphere: A marker for product gas injection due to chlorine-containing very short lived substances. *Geophysical Research Letters*, 46(2), 1032–1039. <https://doi.org/10.1029/2018GL079784>

Hersbach, H., Bell, B., Berrisford, P., Hirahara, S., Horányi, A., Muñoz Sabater, J., et al. (2020). The ERA5 global reanalysis. *Quarterly Journal of the Royal Meteorological Society*, 146, 1999–2049. <https://doi.org/10.1002/qj.3803>

Highwood, E. J., & Hoskins, B. J. (1998). The tropical tropopause. *Quarterly Journal of the Royal Meteorological Society*, 124(549), 1579–1604.

Hoffmann, L., Günther, G., Li, D., Stein, O., Wu, X., Griessbach, S., et al. (2019). From ERA-Interim to ERA5: the considerable impact of ECMWF’s next-generation reanalysis on Lagrangian transport simulations. *Atmospheric Chemistry and Physics*, 19(5), 3097–3124. <http://doi.org/10.5194/acp-19-3097-2019>

Hossaini, R., Chipperfield, M. P., Montzka, S. A., Leeson, A. A., Dhomse, S. S., & Pyle, J. A. (2017). The increasing threat to stratospheric ozone from dichloromethane. *Nature Communications*, 8, 15962. <https://doi.org/10.1038/ncomms15962>

Hossaini, R., Chipperfield, M. P., Montzka, S. A., Rap, A., Dhomse, S., & Feng, W. (2015). Efficiency of short-lived halogens at influencing climate through depletion of stratospheric ozone. *Nature Geoscience*, 8(3), 186. <https://doi.org/10.1038/NGEO2363>

Hossaini, R., Patra, P. K., Leeson, A. A., Krysztofiak, G., Abraham, N. L., Andrews, S. J., et al. (2016). A multi-model intercomparison of halogenated very short-lived substances (TransCom-VSLs): Linking oceanic emissions and tropospheric transport for a reconciled estimate of the stratospheric source gas injection of bromine. *Atmospheric Chemistry and Physics*, 16, 9163–9187. <https://doi.org/10.5194/acp-16-9163-2016>

- Jensen, E. J., Pfister, L., Jordan, D. E., Bui, T. V., Ueyama, R., Singh, H. B., et al. (2017). The NASA Airborne Tropical Tropopause Experiment: High-altitude aircraft measurements in the tropical western Pacific. *Bulletin of the American Meteorological Society*, 98(1), 129–143. <https://doi.org/10.1175/BAMS-D-14-00263.1>
- Kaiser, J., Engel, A., Borchers, R., & Röckmann, T. (2006). Probing stratospheric transport and chemistry with new balloon and aircraft observations of the meridional and vertical N<sub>2</sub>O isotope distribution. *Atmospheric Chemistry and Physics*, 6(11), 3535–3556. <https://doi.org/10.5194/acp-6-3535-2006>
- Kim, J., Li, S., Kim, K. R., Stohl, A., Mühle, J., Kim, S. K., et al. (2010). Regional atmospheric emissions determined from measurements at Jeju Island, Korea: Halogenated compounds from China. *Geophysical Research Letters*, 37(12), 2007–2011. <https://doi.org/10.1029/2010GL043263>
- Konopka, P., Ploeger, F., & Müller, R. (2012). Entropy-based and static stability based Lagrangian model grids. In *Lagrangian modeling of the atmosphere*, geophysical monograph series, 200, AGU Chapman Conference on Advances in Lagrangian Modeling of the Atmosphere. Vols. 9–14. Grindelwald, Switzerland.
- Laube, J. C., Engel, A., Bönisch, H., Möbius, T., Sturges, W. T., Braß, M., & Röckmann, T. (2010a). Fractional release factors of long-lived halogenated organic compounds in the tropical stratosphere. *Atmospheric Chemistry and Physics*, 10(3), 1093–1103. <https://doi.org/10.5194/acp-10-1093-2010>
- Laube, J. C., Engel, A., Bönisch, H., Möbius, T., Worton, D. R., Sturges, W. T., et al. (2008). Contribution of very short-lived organic substances to stratospheric chlorine and bromine in the tropics—A case study. *Atmospheric Chemistry and Physics*, 8(23), 7325–7334. <https://doi.org/10.5194/acp-8-7325-2008>
- Laube, J. C., Keil, A., Bönisch, H., Engel, A., Röckmann, T., Volk, C. M., & Sturges, W. T. (2013). Observation-based assessment of stratospheric fractional release, lifetimes, and ozone depletion potentials of ten important source gases. *Atmospheric Chemistry and Physics*, 13(5), 2779–2791. <https://doi.org/10.5194/acp-13-2779-2013>
- Laube, J. C., Martinerie, P., Witrant, E., Blunier, T., Schwander, J., Brenninkmeijer, C. A. M., et al. (2010b). Accelerating growth of HFC-227ea (1,1,1,2,3,3,3- heptafluoropropane) in the atmosphere. *Atmospheric Chemistry and Physics*, 10(13), 5903–5910. <https://doi.org/10.5194/acp-10-5903-2010>
- Laube, J. C., Mohd Hanif, N., Martinerie, P., Gallacher, E., Fraser, P. J., Langenfelds, R., et al. (2016). Tropospheric observations of CFC-114 and CFC-114a with a focus on long-term trends and emissions. *Atmospheric Chemistry and Physics*, 16(23), 15347–15358. <https://doi.org/10.5194/acp-16-15347-2016>
- Leedham Elvidge, E., Bönisch, H., Brenninkmeijer, C. A. M., Engel, A., Fraser, P. J., Gallacher, E., et al. (2018). Evaluation of stratospheric age of air from CF<sub>4</sub>, C<sub>2</sub>F<sub>6</sub>, C<sub>3</sub>F<sub>8</sub> CHF<sub>3</sub>, HFC-125, HFC-227ea and SF<sub>6</sub>; implications for the calculations of halocarbon lifetimes, fractional release factor. *Atmospheric Chemistry and Physics*, 18(5), 3369–3385. <https://doi.org/10.5194/acp-18-3369-2018>
- Leedham Elvidge, E. C., Oram, D. E., Laube, J. C., Baker, A. K., Montzka, S. A., Humphrey, S., et al. (2015). Increasing concentrations of dichloromethane, CH<sub>2</sub>Cl<sub>2</sub>, inferred from CARIBIC air samples collected 1998–2012. *Atmospheric Chemistry and Physics*, 15(4), 1939–1958. <https://doi.org/10.5194/acp-15-1939-2015>
- Legras, B., & Bucci, S. (2020). Confinement of air in the Asian monsoon anticyclone and pathways of convective air to the stratosphere during the summer season. *Atmospheric Chemistry and Physics*, 20, 11045–11064. <https://doi.org/10.5194/acp-20-11045-2020>
- Li, Q., Jiang, J. H., Wu, D. L., Read, W. G., Livesey, N. J., Waters, J. W., et al. (2005). Convective outflow of South Asian pollution: A global CTM simulation compared with EOS MLS observations. *Geophysical Research Letters*, 32(14), 1–4. <https://doi.org/10.1029/2005GL022762>
- Li, D., Vogel, B., Müller, R., Bian, J., Günther, G., Ploeger, F., et al. (2020). Dehydration and low ozone in the tropopause layer over the Asian monsoon caused by tropical cyclones: Lagrangian transport calculations using ERA-Interim and ERA5 reanalysis data. *Atmospheric Chemistry and Physics*, 20(7), 4133–4152. <https://doi.org/10.5194/acp-20-4133-2020>
- Lunt, M. F., Park, S., Li, S., Henne, S., Manning, A. J., Ganesan, A. L., et al. (2018). Continued emissions of the ozone-depleting substance carbon tetrachloride from eastern Asia. *Geophysical Research Letters*, 45(20), 11423–11430. <https://doi.org/10.1029/2018GL079500>
- McCulloch, A. (2017). *Dichloromethane in the environment, A note prepared for the European chlorinated solvents association (ECSA) and the halogenated solvents Industry Alliance (HSIA)*. Retrieved from <http://www.chlorinated-solvents.eu/images/Documents/Newsroom/Dichloromethanepaper.pdf>
- McKenna, D. S. (2002). A new Chemical Lagrangian Model of the Stratosphere (CLaMS) I. Formulation of advection and mixing. *Journal of Geophysical Research*, 107(D16), ACH 15-1–ACH 15-15. <https://doi.org/10.1029/2000JD000114>
- Newman, P. A., Daniel, J. S., Waugh, D. W., & Nash, E. R. (2007). A new formulation of equivalent effective stratospheric chlorine (EESC). *Atmospheric Chemistry and Physics*, 7(17), 4537–4552. <https://doi.org/10.5194/acp-7-4537-2007>
- Oram, D. E., Ashfold, M. J., Laube, J. C., Gooch, L. J., Humphrey, S., Sturges, W. T., et al. (2017). A growing threat to the ozone layer from short-lived anthropogenic chlorocarbons. *Atmospheric Chemistry and Physics*, 17(19), 11929–11941. <https://doi.org/10.5194/acp-17-11929-2017>
- Orbe, C., Waugh, D. W., & Newman, P. A. (2015). Air-mass origin in the tropical lower stratosphere: The influence of Asian boundary layer air. *Geophysical Research Letters*, 42(10), 4240–4248. <https://doi.org/10.1002/2015GL063937>
- Orbe, C., Waugh, D. W., Newman, P. A., & Steenrod, S. (2016). The transit-time distribution from the Northern Hemisphere midlatitude surface. *Journal of the Atmospheric Sciences*, 73(10), 3785–3802. <http://doi.org/10.1175/jas-d-15-0289.1>
- Ostermüller, J., Bönisch, H., Jöckel, P., & Engel, A. (2017). A new time-independent formulation of fractional release. *Atmospheric Chemistry and Physics*, 17(6), 3785–3797. <https://doi.org/10.5194/acp-17-3785-2017>
- Pan, L. L., Atlas, E. L., Salawitch, R. J., Honomichl, S. B., Bresch, J. F., Randel, W. J., et al. (2017). The convective transport of active species in the tropics (contrast) experiment. *Bulletin of the American Meteorological Society*, 98(1), 106–128. <https://doi.org/10.1175/BAMS-D-14-00272.1>
- Pan, L. L., Honomichl, S. B., Kinnison, D. E., Abalos, M., Randel, W. J., Bergman, J. W., & Bian, J. (2016). Transport of chemical tracers from the boundary layer to stratosphere associated with the dynamics of the Asian summer monsoon. *Journal of Geophysical Research: Atmospheres*, 121(23), 14159–14174. <https://doi.org/10.1002/2016JD025616>
- Park, M., Randel, W. J., Emmons, L. K., Bernath, P. F., Walker, K. A., & Boone, C. D. (2008). Chemical isolation in the Asian monsoon anticyclone observed in Atmospheric Chemistry Experiment (ACE-FTS) data. *Atmospheric Chemistry and Physics*, 8(3), 757–764. <https://doi.org/10.5194/acp-8-757-2008>
- Park, M., Randel, W. J., Emmons, L. K., & Livesey, N. J. (2009). Transport pathways of carbon monoxide in the Asian summer monsoon diagnosed from Model of Ozone and Related Tracers (MOZART). *Journal of Geophysical Research*, 114(8), 1–11. <https://doi.org/10.1029/2008JD010621>
- Park, M., Randel, W. J., Gettelman, A., Massie, S. T., & Jiang, J. H. (2007). Transport above the Asian summer monsoon anticyclone inferred from Aura microwave limb sounder tracers. *Journal of Geophysical Research*, 112(16), 1–13. <https://doi.org/10.1029/2006JD008294>



- Ploeger, F., Gottschling, C., Griessbach, S., Grooß, J.-U., Guenther, G., Konopka, P., et al. (2015). A potential vorticity-based determination of the transport barrier in the Asian summer monsoon anticyclone. *Atmospheric Chemistry and Physics*, *15*(22), 13145–13159. <https://doi.org/10.5194/acp-15-13145-2015>
- Ploeger, F., Konopka, P., Günther, G., Grooß, J.-U., & Müller, R. (2010). Impact of the vertical velocity scheme on modeling transport in the tropical tropopause layer. *Journal of Geophysical Research*, *115*(D3), D03301. <https://doi.org/10.1029/2009JD012023>
- Ploeger, F., Konopka, P., Walker, K., & Riese, M. (2017). Quantifying pollution transport from the Asian monsoon anticyclone into the lower stratosphere. *Atmospheric Chemistry and Physics*, *17*(11), 7055–7066. <https://doi.org/10.5194/acp-17-7055-2017>
- Plumb, I. C., Vohralik, P. F., & Ryan, K. R. (1999). Normalization of correlations for atmospheric species with chemical loss. *Journal of Geophysical Research*, *104*(D9), 11723–11732. <https://doi.org/10.1029/1999JD900014>
- Pommrich, R., Müller, R., Grooß, J.-U., Konopka, P., Ploeger, F., Vogel, B., et al. (2014). Tropical troposphere to stratosphere transport of carbon monoxide and long-lived trace species in the Chemical Lagrangian Model of the Stratosphere (CLaMS). *Geoscientific Model Development*, *7*, 2895–2916. <https://doi.org/10.5194/gmd-7-2895-2014>
- Randel, W. J., & Park, M. (2006). Deep convective influence on the Asian summer monsoon anticyclone and associated tracer variability observed with Atmospheric Infrared Sounder (AIRS). *Journal of Geophysical Research*, *111*(12), 1–13. <https://doi.org/10.1029/2005JD006490>
- Randel, W. J., Park, M., Emmons, L., Kinnison, D., Bernath, P., Walker, K. A., et al. (2010). Asian monsoon transport of pollution to the stratosphere. *Science*, *328*(5978), 611–613. <https://doi.org/10.1126/science.1182274>
- Say, D., Ganesan, A. L., Lunt, M. F., Rigby, M., O'Doherty, S., Harth, C., et al. (2019). Emissions of halocarbons from India inferred through atmospheric measurements. *Atmospheric Chemistry and Physics*, *19*(15), 9865–9885. <https://doi.org/10.5194/acp-19-9865-2019>
- Sinnhuber, B. M., Sheode, N., Sinnhuber, M., Chipperfield, M. P., & Feng, W. (2009). The contribution of anthropogenic bromine emissions to past stratospheric ozone trends: A modelling study. *Atmospheric Chemistry and Physics*, *9*(8), 2863–2871. <https://doi.org/10.5194/acp-9-2863-2009>
- Tissier, A.-S., & Legras, B. (2016). Convective sources of trajectories traversing the tropical tropopause layer. *Atmospheric Chemistry and Physics*, *16*, 3383–3398. <https://doi.org/10.5194/acp-16-3383-2016>
- Umezawa, T., Baker, A. K., Oram, D., Sauvage, C., O'Sullivan, D., Rauthe-Schöch, A., et al. (2014). Methyl chloride in the upper troposphere observed by the CARIBIC passenger aircraft observatory: Large-scale distributions and Asian summer monsoon outflow. *Journal of Geophysical Research: Atmospheres*, *119*(9), 5542–5558. <https://doi.org/10.1002/2013JD021396>
- Vogel, B., Günther, G., Müller, R., Grooß, J.-U., Afchine, A., Bozem, H., et al. (2016). Long-range transport pathways of tropospheric source gases originating in Asia into the northern lower stratosphere during the Asian monsoon season 2012. *Atmospheric Chemistry and Physics*, *16*(23), 15301–15325. <https://doi.org/10.5194/acp-16-15301-2016>
- Vogel, B., Günther, G., Müller, R., Grooß, J.-U., Hoor, P., Krämer, M., et al. (2014). Fast transport from Southeast Asia boundary layer sources to northern Europe: Rapid uplift in typhoons and eastward eddy shedding of the Asian monsoon anticyclone. *Atmospheric Chemistry and Physics*, *14*(23), 12745–12762. <https://doi.org/10.5194/acp-14-12745-2014>
- Vogel, B., Günther, G., Müller, R., Grooß, J.-U., & Riese, M. (2015). Impact of different Asian source regions on the composition of the Asian monsoon anticyclone and of the extratropical lowermost stratosphere. *Atmospheric Chemistry and Physics*, *15*(23), 13699–13716. <https://doi.org/10.5194/acp-15-13699-2015>
- Vogel, B., Müller, R., Günther, G., Spang, R., Hanumanthu, S., Li, D., et al. (2019). Lagrangian simulations of the transport of young air masses to the top of the Asian monsoon anticyclone and into the tropical pipe. *Atmospheric Chemistry and Physics*, *19*, 6007–6034. <https://doi.org/10.5194/acp-19-6007-2019>
- Volk, C. M., Elkins, J. W., Fahey, D. W., Dutton, G. S., Gilligan, J. M., Loewenstein, M., et al. (1997). Evaluation of source gas lifetimes from stratospheric observations. *Journal of Geophysical Research*, *102*(D21), 25543–25564. <https://doi.org/10.1029/97JD02215>
- Vollmer, M. K., Rigby, M., Laube, J. C., Henne, S., Siek, T., Gooch, L. J., et al. (2015). Abrupt reversal in emissions and atmospheric abundance of HCFC-133a (CF<sub>3</sub>CH<sub>2</sub>Cl). *Geophysical Research Letters*, *42*, 8702–8710. <https://doi.org/10.1002/2015GL065846>
- Yan, X., Konopka, P., Ploeger, F., Wright, J. S., Wright, J. S., Müller, R., & Riese, M. (2019). The efficiency of transport into the stratosphere via the Asian and North American summer monsoon circulations. *Atmospheric Chemistry and Physics*, *19*(24), 15629–15649. <https://doi.org/10.5194/acp-19-15629-2019>